Polymer Testing 138 (2024) 108556

Contents lists available at ScienceDirect

Polymer Testing

journal homepage: www.elsevier.com/locate/polytest

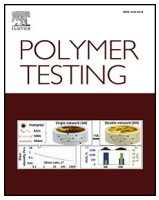

Upgrading properties and circularity of the recycled flexible polypropylene by developing composites with an optimal combination of a fumed silica and maleated polypropylene copolymer: Influence of the addition of copolymer, type of fumed silica and the silica/copolymer ratio on packaging properties

Eliezer Velásquez [a,b,*], Carol López-de-Dicastillo [c], Cristian Patiño Vidal [d,e], Guillermo Copello [f,g], C.J. Pérez [h], Abel Guarda [a,b,i], María José Galotto [a,b,i]

[a] Packaging Innovation Center (LABEN-Chile), University of Santiago of Chile (USACH), Santiago, 9170201, Chile
[b] Center for the Development of Nanoscience and Nanotechnology (CEDENNA), University of Santiago of Chile (USACH), Santiago, 9170124, Chile
[c] Packaging Laboratory, Institute of Agrochemistry and Food Technology (IATA) -CSIC, 46980, Paterna, Spain
[d] Universidad Nacional de Chimborazo (UNACH), Faculty of Engineering, Safety and Resources Valorization Research Group (INVAGRO), Av. Antonio José de Sucre Km 1 1/2, Riobamba, Ecuador
[e] Group for Research and Innovation in Food Packaging, Riobamba, Ecuador
[f] Universidad de Buenos Aires. Facultad de Farmacia y Bioquímica. Departamento de Ciencias Químicas. Buenos Aires, Argentina
[g] CONICET - Universidad de Buenos Aires. Instituto de Química y Metabolismo del Fármaco (IQUIMEFA), Buenos Aires, Argentina
[h] Institute of Materials Science and Technology (INTEMA), National University of Mar del Plata-National Research Council (CONICET), Argentina
[i] University of Santiago of Chile (USACH), Technological Faculty, Food Science and Technology Department (DECYTAL), Chile

ARTICLE INFO

Keywords:
Recycling
Food packaging
Flexible polypropylene
Nanocomposite
Fumed silica
Maleated polypropylene

ABSTRACT

Rigid polypropylene is mechanically recycled but flexible polypropylene is mostly used in energetic valorization because of the poor properties of the recycled polymer. A recycled polypropylene-based composite with outstanding properties for flexible food packaging was developed. For the first time, the influence of maleated polypropylene copolymer addition and the fumed silica/copolymer ratio on the packaging properties of recycled flexible polypropylene under the effects of silica hydrophilicity was investigated. The structural, morphological, thermal, mechanical, melt flow, overall migration, water vapor barrier and sealing properties of the developed nanocomposites were analyzed. Prominently, the addition of 1:1 maleated polypropylene and hydrophobic nanosilica improved the global performance of all tested methods. The recycled polypropylene had an overall migration to olive oil of 17 mg dm^{-2}, exceeding the limit allowed for food packaging, but the developed added-value composite reduced it to the tolerance limit according EU legislation. The seal strength was drastically increased by 50 % with adhesive peeling, high thermal stability, and well-dispersed particles without affecting the ductility.

1. Introduction

Flexible packaging "business-to-consumer" (B2C) comprises any flexible packaging used and discarded by an individual within a home or on the go. According to the Ellen MacArthur Foundation, flexible packaging is growing faster than other plastic packaging categories (5 % annual growth globally from 2019 to 2020). It encompasses the market with more challenges to address toward sustainability. These materials are primarily single-use and have very low recycling rates [1]. Currently, very few flexible plastics B2C are recycled anywhere globally, with recycling rates lower than 8 % in Europe and nearly 0 % worldwide [2].

The recycling of flexible plastics involves losses of quantity and quality deterioration; therefore, virgin raw polymer input is needed. Thus, only a fraction of the flexible packaging is recirculated into high-quality products. In addition, virgin polymer input requirements for

* Corresponding author. Packaging Innovation Center (LABEN-Chile), University of Santiago of Chile (USACH), Santiago 9170201, Chile.
E-mail address: eliezer.velasquez@usach.cl (E. Velásquez).

https://doi.org/10.1016/j.polymertesting.2024.108556
Received 19 May 2024; Received in revised form 6 August 2024; Accepted 22 August 2024
Available online 23 August 2024

food packaging are greater because of the challenge of developing materials from recycled packaging that can be used in food contact [3].

One of the plastics widely used in flexible packaging is polypropylene (PP), an expensive thermoplastic polymer with exceptional characteristics, such as thermal resistance, humidity barrier, lightweight, recyclability, and processability with the typical industrial equipment for plastic conversion [4]. The PP packaging film market has experienced a growing demand for bendy and lightweight sustainable packaging solutions, and manufacturers are focused on developing high-performance recyclable PP films. The global PP packaging film marketplace is estimated to exhibit a CAGR of 6.78 % from 2023 to 2030 [5]. Consequently, increasing PP film recycling rates is needed to diminish PP film accumulation in ecosystems and achieve more circular production.

Mechanical recycling is a waste recovery strategy for reducing plastic waste because it is easily implementable and does not require expensive or complex modification of the manufacturing equipment. Nonetheless, mechanical recycling of polymers causes polymer degradation reactions and property loss [6,7]. Thermal-mechanical reprocessing of PP results in reactions such as chain scission and hydroperoxide formation, which deteriorate the properties of the polymer [8,9]. This degradation phenomenon is worsened through cross-contamination during recycling, and the tensile strength, thermal stability, impact strength, barrier ability, and seal strength, among other properties, are modified [8,10]. In the case of food packaging applications, even more critical is that the migration of substances from recycled PP waste to food could increase because of by-side products, oligomers, pollutants incorporated during recollection and other substances of low molar mass produced during thermal-mechanical reprocessing [11].

On the other hand, polymer nanocomposite development has been increasing to tune polymer performance for several applications [12–14]. Nanotechnology has been used to improve the properties of PP, mainly by testing virgin resin and several nanofillers, such as nanoclays, carbon nanotubes, and graphene nanoplatelets [14,15]. In contrast, fumed silica has rarely been investigated in plastic packaging waste. Fumed nanosilica (NS) is an amorphous synthetic silica thermally synthesized as a white powder without odor, non-toxic, inexpensive, commercially available, and authorized as a food additive [16,17]. This silica has a high specific surface area and can be hydrophobized by chemical modification to tune interactions with neighboring components. Nonetheless, the use of NS in recycled flexible polypropylene from plastic waste streams needs to be studied in order to address several challenges associated with plastic's properties for food packaging applications. For example, overall migration to food simulants requires investigation because overall migration values have been reported to overcome the established limit in some recycled plastics [11,18–20] and because of the quality of the seal strength of the film for flexible packaging. Besides, the suitability of the properties of nanocomposites for food packaging depends on the type of polymer, type and concentration of the nanofiller, additives and compatibilizers; and must be studied case by case according to the European Food Safety Authority [21]. PP graft copolymers have been used as coupling agents between polyolefins and natural fillers. In this context, acid-modified polyolefins such as PP and polyethylene graft copolymers with maleic anhydride with segments that interact with the hydrophobic polymer and with natural fillers have been studied [22–24]. They have mostly been studied to enhance mechanical properties, but fumed silica/MAPP as simultaneous modifiers of seal ability and overall migration behavior have not been reported.

These factors encourage the development and testing of polymer composite systems based on recycled flexible polypropylene for more sustainable production and the circular transformation of plastic management [25] and contribute to the sustainable development goals of the United Nations, which are associated with prevention, reduction, recycling, and reuse strategies to reduce waste generation by 2030 (UN, Responsible Consumption and Production, Sustainable Development Goals, Goal 12.5).

This research developed an added-value nanocomposite with outstanding properties based on recycled flexible PP and NS by incorporating maleated polypropylene (MAPP), a copolymer that acted as a compatibilizer. The recycled flexible polypropylene emulated post-consumer conditions by a post-industrially controlled collection of discarded food packaging. For the first time, the influence of the NS/MAPP mass ratio on PCPP properties was revealed under the effects of NS type. Two types of fumed silica, hydrophilic and dimethyldichlorosilane-treated, were used at different mass ratios of the maleated polypropylene compatibilizer and the fumed silica. The performance of the developed packaging polymer materials was tested by analyzing their structural (ATR-FTIR), morphological (SEM–EDS), thermal (DSC/TGA), and tensile properties, melt flow rate, seal strength, water vapor permeability and overall migration to olive oil for food packaging applications.

2. Materials and methods

2.1. Polymers and nanofillers

Virgin polypropylene homopolymer in pellets (VPP) (MFR = 3 g 10 min^{-1}) was obtained from Petroquim S.A., Chile. Recycled polypropylene (MFR = 6.8 g 10 min^{-1}) in pellets (PCPP) from flexible packaging was purchased from Inproplas S.A. (Chile). The recycled flexible polypropylene emulates post-consumer recycled plastic because it was obtained from discarded flexible packaging that was in contact with food but collected by a post-industrial-controlled process without going to the market or being disposed of at waste collection points where there is a critical contamination risk. Polypropylene-*g*-maleic anhydride, maleated polypropylene (MAPP) pellets ($\overline{M}_w$ = 9100 and $\overline{M}_n$ = 3900 Da, MFR non-measurable because of high flowability) contained between 8 and 10 wt% maleic anhydride (Sigma–Aldrich). Two commercial fumed silicas (hydrophilic and hydrophobized) were purchased from Haochuang Material (native particle size: 5 nm–40 nm): hydrophilic nanosilica (NS1), specific surface area = 200 m^2 g^{-1}, and the chemically treated with dimethyldichlorosilane nanosilica (NS2).

2.2. Obtention of the nanocomposites

Nanocomposites were prepared in a Labtech Scientific LTE-20–40 twin-screw extruder (Samutprakarn, Thailand). After homogenization, a blend of PCPP and MAPP in pellets and NS in powder was fed to the hoppers. The recycled polymer and nanofiller were previously dried at 100 °C for 24 h. The extrusion profile was between 180 °C (feeding zone) and 195 °C (flat die). Nanocomposites with NS1 and NS2 were developed in pellets and film formats to study different MAPP interactions. First, for pellet production, threads were obtained at a 35 rpm screw speed (torque: 43 %) using a round nozzle die. Then, the threads were immersed in a water bath (Scientific Model LW-100, Bangkok, Thailand) and cut at 10 m min^{-1} in a pelletizer (Scientific, LZ-120, Bangkok, Thailand). For film production at the same screw speed, the torque was between 42 % and 57 %, and the chilling roller velocities were between 1.7 and 1.4 m min^{-1}. The mass concentrations in the nanocomposite were 1 wt% NS and 1 and 3 wt% MAPP. The nanocomposite films were named PCPP-XNSY-MAPPZ, where Y is the type of fumed silica (1: hydrophilic and 2: hydrophobized) and X and Z are the weight fractions of NS and MAPP, respectively. Besides, PCPP and VPP controls in pellets and film formats were produced under the same extrusion conditions (Table 1). VPP is an isotactic PP used to manufacture bio-oriented films by extrusion or coextrusion and is a commercial reference polymer for related applications. The films had thicknesses between 150 and 230 μm.

Table 1
Composition of the samples.

Film	Mass Percentage (%)				
	VPP	PCPP	NS1	NS2	MAPP
PCPP-1NS1-1MAPP	0	98	1	0	1
PCPP-1NS1-3MAPP	0	96	1	0	3
PCPP-1NS2-1MAPP	0	98	0	1	1
PCPP-1NS2-3MAPP	0	96	0	1	3
VPP	100	0	0	0	0
PCPP	0	100	0	0	0
PCPP-1MAPP	0	99	0	0	1
PCPP-3MAPP	0	97	0	0	3
PCPP-1NS1	0	99	1	0	0
PCPP-1NS2	0	99	0	1	0

2.3. Characterization of the nanocomposites

The effects of MAPP addition and the NS:MAPP ratio on PCPP film performance were evaluated via the following testing.

2.3.1. Scanning electron microscopy and energy dispersive spectroscopy (SEM–EDS)

The film surface and NS dispersion were analyzed via ESEM (FEI Quanta-200, FEI, Hillsboro, OR) equipment with an EDS analyzer (Oxford Instruments). The samples were coated with graphite. SEM images and EDS elemental mapping were obtained. ImageJ open-source software was used to measure the particle sizes and lengths from the images (https://imagej.nih.gov/ij/).

2.3.2. Thermal analysis

The films were analyzed via differential scanning calorimetry (DSC) in a Mettler DSC-822e analyzer (Schwarzenbach, Switzerland). Samples (5 mg) in aluminum capsules were subjected to a unique heating program from 0 °C to 250 °C at 10 °C min^{-1} under a N_2 atmosphere. Melting temperatures (T_m) and melting enthalpies (ΔH_m) were recorded. Furthermore, crystalline fraction (X_c) was determined as the melting enthalpy of the specimen (ΔH_m) divided by the product of the melting enthalpy of 100 % crystalline polypropylene ($\Delta H_{100} = 207$ J g^{-1}) [26] and the mass fraction of the polymer in the nanocomposite (X_{PP}). The X_{PP} was estimated by subtracting the masses of the NS and MAPP from the mass of the sample, neglecting pollutants in the recycled polymer.

The decomposition initiation (T_{onset} at 2.5 % mass loss) and maximum degradation rate (T_d) temperatures were determined through thermogravimetric analysis (TGA) using a TGA/DSC 1 analyzer (Schwarzenbach, Switzerland). Each film (5 mg) was collocated in alumina capsules. The heating program ranged from 30 °C to 700 °C at 10 °C min^{-1} and 50 mL min^{-1} N_2 flow.

2.3.3. Melt flow rate (MFR) and zero-shear rate viscosity

The MFR was measured using a Zwick-Roell Mflow plastometer (Ulm, Germany) according to the ASTM D1238-20 standard. The pellets (6 g) were subjected to 230 °C and a piston (2.16 kg). The samples were preheated at the setting temperature for 7 min. Six MFI replicates were obtained for each sample.

The zero-shear rate viscosity of the samples was obtained from complex viscosity curves by rheological analysis in a parallel plate rheometer Anton Paar MCR301. Polymeric plates from the pellet samples were injection molded following the procedure reported in previous work [27]. The complex viscosity versus frequency curves were obtained at 190 °C under a nitrogen atmosphere in dynamic mode. The frequency was between 0.1 and 500 rad s^{-1} and corresponded to the linear viscoelastic range according to previous amplitude sweep tests for polypropylene.

2.3.4. Tensile properties

Young's modulus (E), tensile strength (σ_B), and elongation at break (ε_B) were measured according to the ASTM D882 normative in a universal machine Zwick Roell Proline BDO-FB 0.5 TH (Ulm, Germany) with a load cell of 500 N. Ten specimens of each sample (16 cm × 2.5 cm) were cut and conditioned at 23 °C and 50 % relative humidity (RH) for 48 h according to the ASTM standard D618 for thin sheeting. Initially, the clamps were separated by 50 mm, and the test was carried out at 500 mm min^{-1}.

2.3.5. Seal strength (SS)

Films (16 cm × 2.5 cm) were sealed using a Labthink HST-H3 sealing machine (Medford, OR, USA) according to the ASTM F2029 standard. The sealing temperature, time and pressure were 153 °C, 2.5 s and 350 kPa, respectively, based on the optimum sealing conditions reported for this type of post-consumer polypropylene [18]. The sealed films were conditioned at 50 % RH for 48 h. Subsequently, the SS of the nanocomposites was determined with the universal machine described in the above section according to the non-supported seal technique of the ASTM F88/F88 M − 21 normative. The distance between clamps was 25 mm, and the crosshead speed was 250 mm min^{-1}. Six measurements for each sample were averaged to report SS. For each replicate, the SS was calculated as the average of the values plotted within 80 % of the central range of the sealing curve using TestXpert III software.

2.3.6. Overall migration (OM)

OM assays were carried out according to EU Regulation N° October 2011 [20]. Olive oil (maximum acidity of 0.3 %) was selected in order to promote maximum OM from the plastic because of the hydrophobic nature of PP, which has an expected greater affinity for a fatty simulant. The film was maintained in contact by immersion in olive oil for 10 days at 40 °C. Finished this time, the sample was withdrawn and cleaned to remove the excess oil. Subsequently, Soxhlet extraction extracted the olive oil possibly absorbed by the sample, and the results were quantified by gas chromatography using calibration curves prepared from methylated extra virgin olive oil solutions. The procedure has been described previously [18]. The OM content was calculated by gravimetry, knowing the initial weight and the weight at the end of the contact time of the films, considering the correction by subtraction of the olive oil determined by Soxhlet extraction in the final sample. OM was determined by averaging two measurements.

2.3.7. Water vapor permeability (WVP)

WVP was reported as the average of two measurements. The water vapor transmission rate (WTR) of the films with a contact area of 5.5 cm^2 was determined at 37.8 °C and 90 % RH with an analyzer Permatran Mocon W 3/34 (Minneapolis, USA) according to the F1249-20 standard normative. Films were put into permeability cells, and the WVTR values were plotted until they obtained a constant value. The thicknesses of the tested films were between 150 μm and 230 μm. The WVP was calculated as the product of the WVTR and the thickness of the film (L) and divided by the gradient of the water vapor partial pressure (P_w).Where WVTR is the water vapor transmission rate (g m^{-2} s^{-1}), L is the thickness of the films (mm), and P_W is the gradient of partial pressure of water vapor (Pa).

2.3.8. Statistical analysis

The X_c, MFR, SS, OM, WVP and tensile properties were statistically analyzed using Statgraphics Plus 5.1. Significant differences between the samples with a confidence level of 95 % ($p < 0.05$) were found by analysis of variance (ANOVA) and Fisher's least significant difference multiple range test. A random experimental design was used. Statistically significant differences among samples were denoted with different superscript letters in the discussion section's reported results.

3. Results and discussions

3.1. Morphological analysis

SEM micrographs of the films at the studied NS:MAPP ratios are shown in Fig. 1. A non-porous and crack-free surface is observed. Topography variations are associated with polymer agglomeration or particles detected even in the control PCPP (Supplemental Information, Fig. S1), which negates the possibility that these observations are related to NS agglomerations. Furthermore, EDS spectra were recorded to confirm the absence of such agglomerations and the relative percentage and homogeneity of the fumed silica particle distribution (Fig. 2). According to EDS elemental mapping, all the nanocomposite films had the same Si amount. Moreover, compared with the nanocomposite, the PCPP films contained a minimum amount of Si due to cross-contamination with this ubiquitous element in the recycled plastic (Supplemental Information, Figs. S2 and S3).

On the other hand, a lower number and smaller size of brighter spots, accounting for zones with a higher density of NS particles, are obtained at an NS:MAPP ratio of 1:3, as shown in Fig. 2. This indicated that the graft copolymer better dispersed the NS into the PCPP. In this regard, the role of MAPP was more significant for nanocomposites with hydrophilic NS1. At the same NS:MAPP ratio, smaller particles and better dispersion are obtained for hydrophobic NS2 because of its increased miscibility with the PCPP matrix. Nonetheless, the addition of 1 wt% MAPP did not reduce the agglomeration observed in EDS images for NS1.

3.2. Thermal analysis

3.2.1. Differential scanning calorimetry

The DSC parameters and the crystallinities of the films are reported in Table 2. PCPP exhibited three melting points at 124 °C, 158 °C and 163 °C. The first melting is attributed to the presence of LDPE, LLDPE, copolymer-grade PP or blends of these materials detected by ATR-FTIR analysis (Supplemental Information, Section S2, Fig. S4) because of cross-contamination with PE or multilayers during the recycling of flexible packaging, considering that the materials have similar specific gravities, in concordance with the findings for recycled polyolefins [28, 29]. The double melting of PCPP is associated with two crystalline structures that melt at 158 °C and 163 °C around the melting point of VPP (162 °C).

Conversely, the lower crystallinity of PCPP than VPP could be related to a combination of several factors: the presence of PE traces impeded the ordering of the PP chains during processing; the shorter polymeric chains caused by recycling produced fewer ordered zones or shorter crystals that required less energy to melt, as could be verified through the enthalpies (Table 2); and the fact that PCPP was not exclusively composed of isotactic type PP like VPP.

The melting temperature of PCPP did not change with the addition of NS or MAPP. However, two shoulders at close temperature values in the melting transition of the PP were detected as related to two crystal regions with different ordering in some samples with MAPP (Table 2).

The incorporation of NS and MAPP resulted in nanocomposites with a thermal behavior similar to that of PCPP, and only a slight increase in crystallinity was statistically significant at an NS2:MAPP ratio of 1:3 due to the greater nucleation effect of NS2 during the preparation of the film. Conversely, the addition of only MAPP tended to increase the crystallinity of the polymer due to the nucleating role of its lower molar mass chains in the PCPP matrix. The high crystallinity of MAPP is related to its ability to crystallize due to the branching of its maleic anhydride chain [30].

3.2.2. Thermogravimetric analysis

PCPP was thermally more stable than VPP was, as evidenced by the higher T_{onset} and T_d values (Table 3) associated with the PE fraction, as verified by DSC analysis (Fig. S4a), considering that LDPE has been reported to have greater thermal stability than PP [31].

On the other hand, the combined incorporation of NS and MAPP

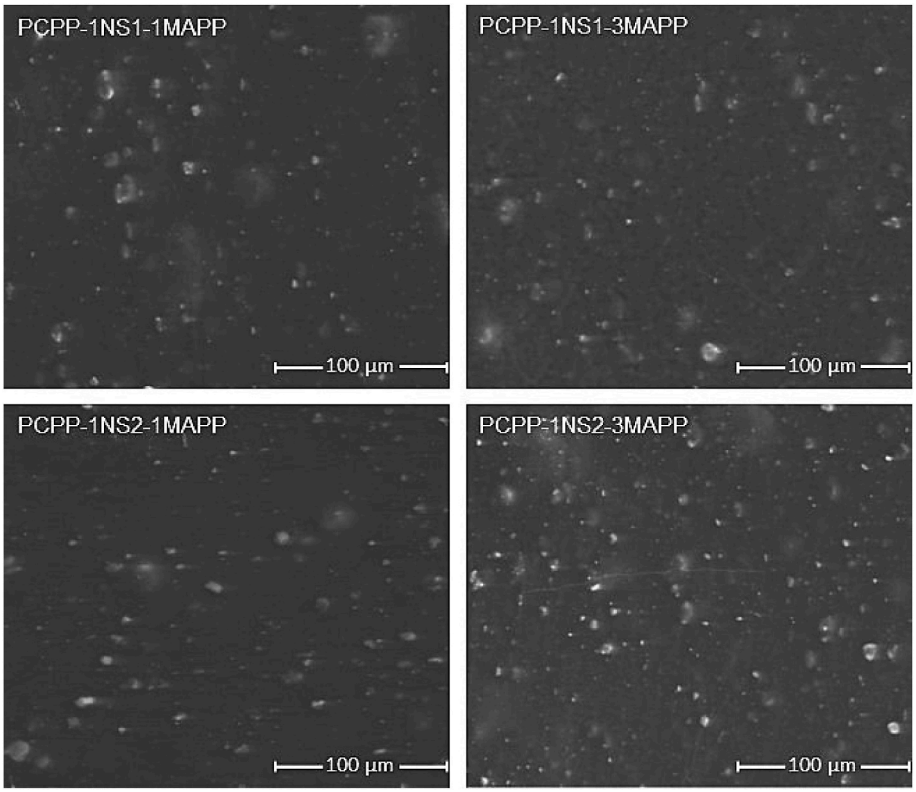

Fig. 1. SEM micrographs of the PCPP-NS-MAPP nanocomposites.

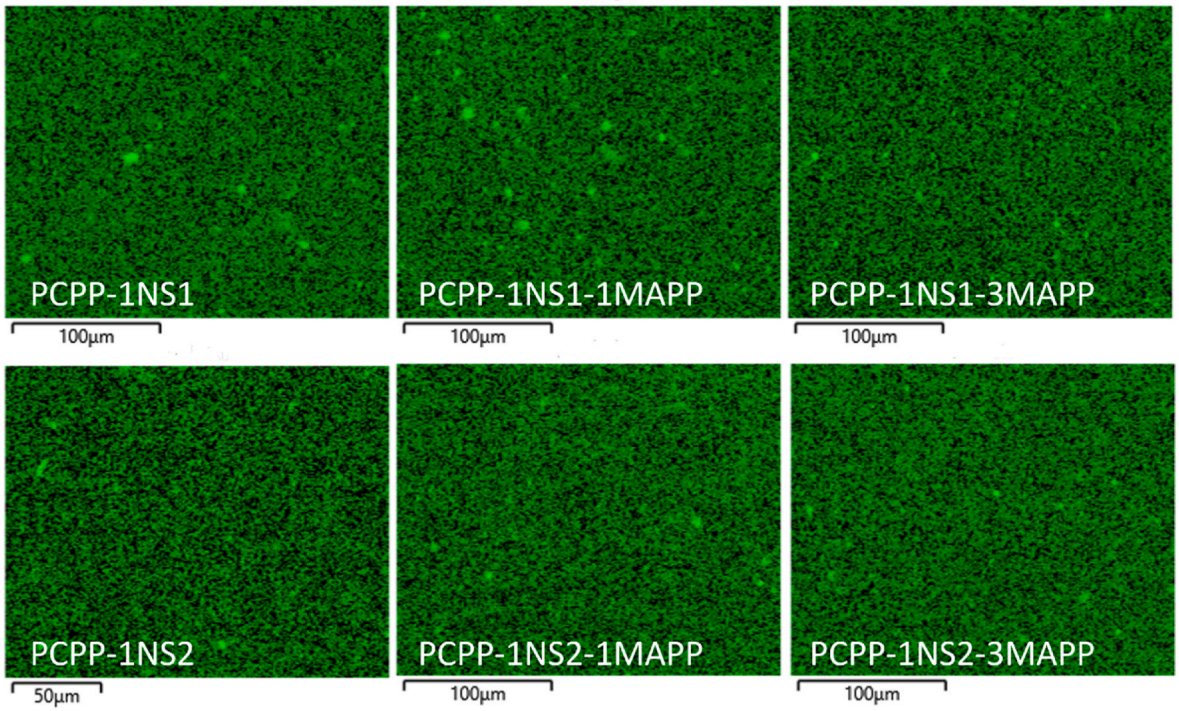

Fig. 2. EDS mapping images of the nanocomposites. Bright spots correspond to fumed silica within the polymer matrix.

Table 2
DSC of the developed films.

Film	Tm_1 (°C)	ΔHm_1 (J/g)	Tm_2 (°C)	Tm_3 (°C)	ΔHm_{2-3} (J/g)	X_c (%)
VPP	–	–	–	162	100.7 ± 1.2	48.7 ± 0.6^{d}
PCPP	124	4.7 ± 0.2	158	163	75.2 ± 0.7	36.5 ± 0.1^{b}
MAPP	–	–	–	154	98.0 ± 3.2	52.6 ± 1.7^{e}
PCPP-1MAPP	124	4.0 ± 0.1	–	163	77.3 ± 0.9	37.7 ± 0.5^{bc}
PCPP-3MAPP		3.9 ± 0.1	162	164	76.8 ± 0.2	38.3 ± 0.1^{bc}
PCPP-1NS1		4.4 ± 0.1	–	162	78.1 ± 1.9	38.1 ± 0.9^{bc}
PCPP-1NS2		3.7 ± 0.1	–	162	69.7 ± 4.2	34.0 ± 2.0^{a}
PCPP-1NS1-1MAPP		4.1 ± 0.1	–	162	75.6 ± 2.9	37.3 ± 1.4^{bc}
PCPP-1NS1-3MAPP		3.9 ± 0.1	160	163	75.1 ± 0.6	37.8 ± 0.3^{bc}
PCPP-1NS2-1MAPP		4.5 ± 0.1	162	163	75.8 ± 0.3	37.4 ± 0.1^{bc}
PCPP-1NS2-3MAPP		4.2 ± 0.1	–	162	78.1 ± 1.2	39.3 ± 0.6^{c}

Significant differences in crystallinity among the samples according to ANOVA and LSD Fischer's test ($p < 0.05$) are indicated by different superscript letters.

increased the thermal stability of PCPP, and the addition of both components increased the thermal stability of the polymer, as evidenced by the greater T_{onset} and T_d concerning control PCPP (Table 3). This is possibly due to i) the high thermal resistance of NS, NS1 not decomposing, and NS2 initiating its loss of mass at 450 °C (Fig. 3) [18] and ii) the interactions between MAPP and PCPP. These interactions that cause a delay in the thermal degradation of PCPP at higher temperatures are evidenced by the greater thermal stability of PCPP-MAPP1 and PCPP-MAPP3 than of control PCPP.

However, at the highest concentration of MAPP, the PCPP-1NS2-3MAPP and PCPP-3MAPP samples produced minor increases in the T_{onset} and T_d of PCPP, correspondingly, because of the early degradation of MAPP. MAPP is a low molar mass copolymer that loses mass at approximately 216 °C due to the degradation of the maleic anhydride group, and a second mass loss at 450 °C is associated with polymer degradation; thus, MAPP is less thermal stable than PP [32,33]. The highest concentration of MAPP did not affect the thermal stability of PCPP-1NS1-3MAPP because NS1 has such high thermal resistance that it did not degrade within the temperature range studied.

Table 3
TGA parameters, MFR, and viscosity of the samples.

Sample	T_{onset} (°C)	T_d (°C)	Zero-shear rate viscosity (Pa s)	MFR (g 10 min^{-1})
VPP	341	433	8646	3.4 ± 0.1^{a}
PCPP	368	454	4420	6.8 ± 0.2^{cd}
PCPP-1NS1-1MAPP	385	464	5444	6.6 ± 0.2^{b}
PCPP-1NS1-3MAPP	383	464	5387	8.6 ± 0.2^{e}
PCPP-1NS2-1MAPP	384	463	4965	6.8 ± 0.2^{d}
PCPP-1NS2-3MAPP	377	463	4670	8.5 ± 0.3^{e}
PCPP-1NS1	385	464	5140	6.6 ± 0.1^{bc}
PCPP-1NS2	387	462	5067	6.7 ± 0.1^{bcd}
PCPP-1MAPP	382	463	–	6.9 ± 0.2^{d}
PCPP-3MAPP	383	459	–	8.4 ± 0.3^{e}
MAPP	216	458	–	–

Significant differences in MFR among the samples according to ANOVA and Fisher's LSD test ($p < 0.05$) are indicated by different superscript letters.

3.3. Melt flow rate and zero-shear rate viscosity

The MFR of the VPP was lower than that of the PCPP. This finding is associated with the lower molar mass of the polymer chains in PCPP resulting from the degradation reactions during shelf life and mechanical recycling and, therefore, the decreased chain entanglement and

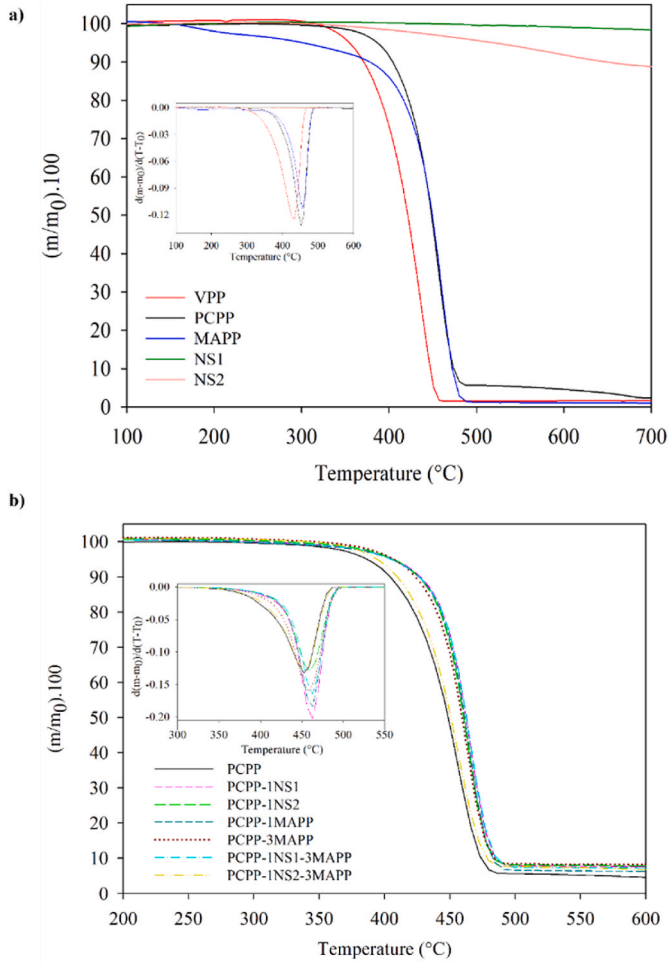

Fig. 3. (a) TGA and (b) DTG curves of the films.

viscosity of the recycled polymer [27] (Table 3).

Samples with NS and MAPP had higher zero-shear rate viscosities than pure PCPP. Nanocomposites with NS1 and MAPP were more viscous than those equivalent to NS2 because the silanol groups of NS1 strongly formed hydrogen-bond interactions with MAPP. Meanwhile, increasing the MAPP concentration tended to reduce the zero-shear rate viscosity when samples with the same type of NS were compared. This could be related to a lowering of the average molar mass of the PP composite with MAPP incorporation, which is in agreement with the trends in complex viscosity at lower shear rates reported for highly filled wood composites based on PP (MFR = 12 g 10 min^{-1}) with and without maleated PP [34]. In concordance, MFR was only increased when 3 wt% MAPP was added, considering this addition implied that a greater fraction of lower molar mass chains composed the sample.

3.4. Tensile properties

The E and σ_M of PCPP were drastically lower than those of commercial VPP-based films (E = 1216 ± 146 MPa, σ_M = 41,1 ± 4,4 MPa), which could be associated with PCPP containing PE, as was verified by DSC and polymer chains of lower molar mass generated during reprocessing, also considering that PCPC was not composed only of recycled VPP used as a reference (Fig. 4). PE is more flexible and is immiscible with PP; thus, stress points are formed between the interphase PP/PE and trigger a lower resistance [19]. Also, a lower PCPP crystallinity than VPP, and shorter polymeric chains in the recycled plastic forming shorter crystalline networks, reduced the stiffness of PCPP [35]. Regarding ε_B, the lower ductility of the PCPP (18.7 ± 6.9 %)

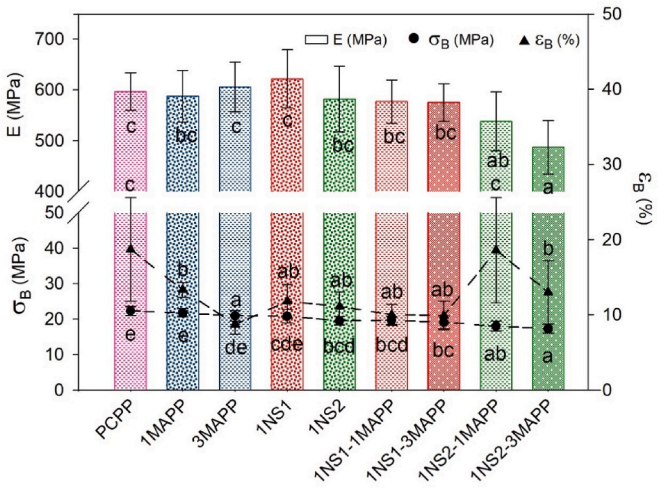

Fig. 4. Tensile properties of the films. Different letters (a, b, c, d, e) indicate significant differences among the samples according to ANOVA and Fisher's LSD test ($p < 0.05$).

compared to VPP (24,6 ± 6,3 %) could be attributed to surface imperfection points partially associated with the difference in compatibility between the PP and pollutants, which caused an earlier break.

Fig. 4 shows that the tensile properties of the nanocomposite films with NS and MAPP tended to be lower than those with PCPP. NS and MAPP, separately added, reduced ε_B with respect to the control PCPP, which was clearly observed at 3 wt% MAPP. The negative effect of the addition of MAPP on the ductility of the PCPP-MAPP samples is associated with an average molar mass reduction caused by this low molar mass copolymer. These shorter chains produced lower chain entanglements. A comparison of the εB values of samples with the same type of NS but different NS:MAPP ratios revealed significant differences between the films with NS2 (Fig. 4). Besides, similarly to PCPP-MAPP samples, the addition of 3 wt% MAPP reduced the elongation ability in the nanocomposites with NS2.

Conversely, when the effect of the NS type on the 1NS:1MAPP ratio was compared, PCPP-1NS2-1MAPP presented the highest elongation but a tendency to reduce E and σ_M. The same phenomenon but with a greater impact on the stiffness and tensile strength was observed for the samples with a 1NS:3MAPP ratio. This could be attributed to MAPP being in excess when 3 wt% was used, which was not needed to make NS2 compatible with MAPP because the nanosilica was already hydrophobized; thus, a plasticizing effect was promoted in accordance with the lowest viscosity for PCPP-1NS2-3MAPP (Table 3). Furthermore, the lower number of agglomerates on the films with NS2 and MAPP, as verified by EDS, reduced the possibility of an earlier break (Fig. 2). The highest deviations in the εB values of the PCPP and PCPP-NS2-MAPP films could be attributed to a greater surface and compositional heterogeneity along the film regarding imperfections or tension points that promote the rupture associated with immiscibility among the components and the pollutants in these samples. The magnitude of the standard deviations among samples depended on the typical compositional heterogeneity of recycled plastics used among different extrusion batches.

The absence of the expected improvement in E and σ_M by NS2 addition without MAPP due to NS2 being hydrophobic and conferring miscibility with the polymer matrix could be associated with issues during extrusion processing, as was evidenced through the lowest crystallinity for this sample according to DSC analysis (Table 2) and superficial and compositional heterogeneities in the recycled material load.

3.5. Seal strength (SS)

All the films exhibited adhesive peeling failures, and a minimum number of the specimens underwent material breakage (Table 4). PCPP had an average SS of 183 N m^{-1}.

Incorporating MAPP or NS separately diminished the SS. Increasing the MAPP concentration significantly reduced the SS because of i) a lower molar mass reduction with a greater proportion of carbonyl groups meanly from MAPP in the polymer blend, which reduced the sealability, and ii) a lower polymer density (higher MFI) because of the maleic anhydride of the MAPP, which is a bulky group located between PP chains, thus preventing PCPP chain interactions and entanglements during seal formation.

A significant reduction in the SS of PCPP-NS1 was obtained because a greater number of weak adhesion sites in the interphase polymer-NS1 were formed after thermosealing due to the hydrophilic nature of NS1, which triggered seal failure. The SS of NS1-based nanocomposites could not be improved through MAPP addition. Meanwhile, the greater miscibility of hydrophobic NS2 with the PP matrix caused better heat transfer and maintained interactions between the components during thermosealing.

Prominently, the simultaneous incorporation of NS2 and MAPP at a 1:1 ratio increased SS of the PCPP by 50 %, indicating that 1:1 was the NS2:MAPP ratio for obtaining a good balance between component interactions and chain mobility, crosslinking chains and strengthening the seal. The NS2 could interconnect polymer chains between methyl groups on its modified surface. In addition, the oxygen groups of maleic anhydride could also interact with polymeric hydroperoxide radicals in recycled plastic. It is essential to mention that standard deviations are typical of this test and could be associated with differences in the fraction and dispersion of the components in the seal area.

3.6. Overall migration

As expected, VPP complied with the limit of OM of 10 mg dm^{-2}, which corresponds to 60 mg kg^{-1} of food that occupies a volume of a cubic package with 6 dm^2 of total area, as established by the EU Normative N° October 2011 (Fig. 5). This result agreed with the overall migration reported for virgin PP in olive oil of 7 mg dm^{-2}, which was higher than in ethanol 10 % (0.29 mg dm^{-2}) and 3 % acetic acid (0.30 mg dm^{-2}) associated with the hydrophobic nature of the PP [22]. On the contrary, PCPP and PCPP-NS nanocomposites overcame that limit, although the addition of only NS caused a slight barrier effect to migration. Overall, the migration of these materials corresponded to oligomers and substances with lower molar masses contained in the recycled material as pollutants or generated during thermal-mechanical reprocessing.

The simultaneous incorporation of NS and MAPP at 1 and 3 wt% significantly reduced the OM of PCPP. This effect had a greater impact

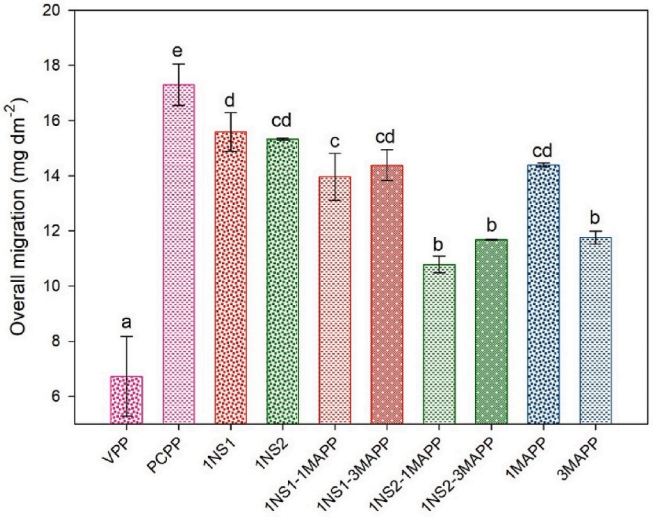

Fig. 5. Overall migration of nanocomposite films to olive oil. Different letters indicate significant differences among the samples according to ANOVA and Fisher's LSD test ($p < 0.05$).

on the PCPP-1NS2-1MAPP nanocomposite when the OM concentration was adjusted (10.8 mg dm^{-2}) to the allowed limit, considering a tolerance level of 3 mg dm^{-2} in fatty simulants. In this case, the better affinity of NS2 for the polymer and the interactions of MAPP with NS2 and PP favored the formation of more tortuous paths that hindered the migration of substances through the plastic film. Besides, oxygen groups in the anhydride maleic in MAPP would be interacting with hydroperoxide radicals or oxidized substances in the recycled PP, inhibiting their migration to the food simulant, as suggested by the decrease in OM with increasing MAPP fraction in the films without NS (Fig. 5).

According to the EU regulation October 2011 [20], simulant D1 shall be chosen as the simulant for testing migration from materials and articles for a certain food category included in the list "Food category specific assignment of food simulants", such as pastry, biscuits, cakes, bread, and other baker's wares, dry (with fatty substances on the surface), chocolate and chocolate-coated products, confectionery products (in solid and paste form, with fatty substances on the surface), processed fruit (fruit preserved in a liquid medium, in an oily medium), dried foods (with fatty substances on the surface), among others.

3.7. Water vapor permeability

The WVP of VPP and PCPP were statistically similar but the incorporation of MAPP or NS significantly increased the WVP (Table 5). This result would be associated with higher hydrophilicity conferred to PP for MAPP and NS, which are molecules containing oxygen functional groups in their chemical structures with higher affinity for water vapor and the

Table 4
Seal strength of the films.

Sample	Seal strength (N m^{-1})	Type of failure
PCPP	183 ± 60^{d}	AP
PCPP-1MAPP	102 ± 68^{bc}	AP
PCPP-3MAPP	28 ± 17^{a}	AP
PCPP-1NS1	43 ± 16^{ab}	AP
PCPP-1NS2	157 ± 108^{cd}	AP (4/6), MB (2/6)
PCPP-1NS1-1MAPP	30 ± 28^{a}	AP (5/6), MB (1/6)
PCPP-1NS1-3MAPP	76 ± 45^{ab}	AP (5/6), MB (1/6)
PCPP-1NS2-1MAPP	278 ± 59^{e}	AP (4/6), MB (2/6)
PCPP-1NS2-3MAPP	164 ± 62^{cd}	AP

Different superscript letters indicate significant differences among the samples according to ANOVA and Fisher's LSD test ($p < 0.05$). Film thicknesses: 150–200 μm. AP: adhesive peel. MB: material break. Total measurements: six for each sample.

Table 5
Water vapor permeability coefficient of the films.

Film	WVP x10^{10} (g mm m^{-2} s^{-1} Pa^{-1})
VPP	0.24 ± 0.06^{a}
PCPP	0.19 ± 0.04^{a}
PCPP-1MAPP	6.28 ± 0.35^{b}
PCPP-3MAPP	6.09 ± 0.16^{b}
PCPP-1NS1	7.75 ± 0.36^{cd}
PCPP-1NS2	8.06 ± 0.30^{de}
PCPP-1NS1-1MAPP	7.34 ± 0.43^{c}
PCPP-1NS1-3MAPP	7.45 ± 0.21^{cd}
PCPP-1NS2-1MAPP	9.73 ± 0.46^{f}
PCPP-1NS2-3MAPP	8.65 ± 0.26^{h}

Different superscript letters indicate significant differences among the samples according to ANOVA and Fisher's LSD test ($p < 0.05$).

formation of voids around NS agglomerations through which water permeates. Besides, MAPP in samples PCPP-MAPP could cause a plasticizing effect by generating free volume between polymer chains because of the maleic anhydride groups, favoring water vapor permeation. Gomez et al. (2015) also evidenced an increase in WVP values of isotactic polypropylene with the increase of loading of spherical silica nanoparticles produced by a sol-gel method, considering the interaction between hydroxyl functional groups of the nanospheres and water vapor phase. The researchers also related the worsening of the water barrier to the generation of voids and permeation channels between adjacent particles due to the agglomerations of nanoparticles [36].

On the other hand, the addition of MAPP within PCPP-NS1 composites did not increase WVP attributed to a partial interaction of the hydroxyl groups of NS1 with the oxygen functional groups of MAPP. Therefore, fewer hydroxyl groups of NS1 would be available to interact with the water vapor. However, a slight increase of the WVP for PCPP-NS2 with the incorporation of MAPP without a clear tendency with MAPP percentage is observed because NS2 is previously hydrophobized and more oxygen functional groups of MAPP are available to interact with water molecules and also plasticize the polymer.

4. Conclusions

The polypropylene-*g*-maleic anhydride copolymer as a compatibilizer and the silica/copolymer ratio had a prominent effect on increasing the seal strength and reducing the overall migration of the recycled flexible polypropylene to the fatty food simulant. The recycled polypropylene exceeded the overall migration limit established by EU legislation for food packaging. Nevertheless, the overall migration was reduced to values near the limit when hydrophobic nanosilica was added with maleated polypropylene or only maleated polypropylene at the highest concentration was incorporated into the film. Surprisingly, the seal strength of the films drastically increased by 52 % when the hydrophobic nanosilica and the compatibilizing copolymer were added at a 1:1 mass ratio. These findings are interesting due to the current need to improve the sealability of polypropylene. In contrast, the seal strength was significantly decreased by the addition of hydrophilic nanosilica due to the weak adhesion sites that formed in the interphase polymer nanosilica. Although the increase of compatibilizing copolymer concentration had an essential role as a dispersion improver of the hydrophilic nanosilica in the polymer matrix, the seal strength was not improved.

On the other hand, the thermal and tensile properties were not significantly affected by the addition of maleated polypropylene copolymer and/or nanosilica, except for the stiffness reduction observed at a mass ratio of 1:3 hydrophobic nanosilica:copolymer, considering that 3 % of the copolymer caused an increase of the melt flow rate. Interestingly, elongation remained invariable when hydrophobic nanosilica and the compatibilizer were simultaneously added at 1:1 the mass ratio, in contrast with the typical reduction in elongation ability, reported when nanofillers are incorporated into polymer matrices. These findings revealed an added-value flexible polypropylene composite that potentially would allow the incorporation and increase of the recycled flexible PP concentration used for new packaging materials. The deviations in the property values of the recycled plastics according to the source which are obtained, their compositional heterogeneity, and the presence of pollutants are challenges to address. Nonetheless, we considered the importance of working with a realistic waste stream to look for the improvement of recycled plastic packaging.

Funding

This work was supported by the "Agencia Nacional de Investigación y Desarrollo" of Chile through the project ANID FONDECYT Initiation N° 11220469.

CRediT authorship contribution statement

Eliezer Velásquez: Writing – review & editing, Writing – original draft, Visualization, Supervision, Project administration, Methodology, Investigation, Funding acquisition, Formal analysis, Conceptualization. **Carol López-de-Dicastillo:** Writing – review & editing, Formal analysis. **Cristian Patiño Vidal:** Writing – original draft, Visualization, Formal analysis, Data curation. **Guillermo Copello:** Writing – review & editing, Formal analysis. **C.J. Pérez:** Writing – review & editing, Formal analysis. **Abel Guarda:** Resources. **María José Galotto:** Resources.

Declaration of competing interest

The authors declare that they have no known competing financial interests or personal relationships that could have appeared to influence the work reported in this paper.

Data availability

Data will be made available on request.

Acknowledgment

Petroquim S.A. (Chile) and INPROPLAS S.A. (Chile) for providing virgin and recycled polypropylene, respectively.

Appendix A. Supplementary data

Supplementary data to this article can be found online at https://doi.org/10.1016/j.polymertesting.2024.108556.

References

[1] Ellen MacArthur Foundation, Flexible packaging: the urgent actions needed to deliver circular economy solutions. https://www.ellenmacarthurfoundation.org/flexible-packaging-the-urgent-actions-needed-to-deliver-circular-economy, 2022 (accessed November 8, 2023).
[2] Brussels, Plastics Recyclers Europe, Flexible Film Market in Europe: State of Play, 2020.
[3] Ellen MacArthur Foundation, Plastic flexibles: design and recycling in the formal sector. https://www.ellenmacarthurfoundation.org/plastic-flexibles-design-and-recycling-in-the-formal-sector, 2022 (accessed November 8, 2023).
[4] A. Alsabri, F. Tahir, S.G. Al-Ghamdi, Environmental impacts of polypropylene (PP) production and prospects of its recycling in the GCC region, Mater Today Proc 56 (2022) 2245–2251, https://doi.org/10.1016/j.matpr.2021.11.574.
[5] Credence Research Report, Polypropylene packaging films Market by Material (Biaxially oriented polypropylene films, cast polypropylene films), by Application (Food & beverage, personal care, pharmaceuticals, industrial packaging, others), and by Distribution Channel (Online segment, supermarkets/Hypermarkets, specialty strores, others). Global Industry Analysis, Size, Share, Growth, Trends, and Forecast Report, Segmented Competitive Landscape and Future Outlook 2017–2030 (2023). https://www.credenceresearch.com/report/polypropylene-packaging-films-market. (Accessed 8 November 2023).
[6] M.S. Nur-A-Tomal, F. Pahlevani, W. Handoko, S.T. Cholake, V. Sahajwalla, Effect of cyclic reprocessing on nylon 12 under injection molding: working toward more efficient recycling of plastic waste, Materials Today Sustainability 11–12 (2021) 100056, https://doi.org/10.1016/j.mtsust.2020.100056.
[7] S. Saikrishnan, D. Jubinville, C. Tzoganakis, T.H. Mekonnen, Thermo-mechanical degradation of polypropylene (PP) and low-density polyethylene (LDPE) blends exposed to simulated recycling, Polym Degrad Stab 182 (2020) 109390, https://doi.org/10.1016/j.polymdegradstab.2020.109390.
[8] Z.O.G. Schyns, M.P. Shaver, Mechanical recycling of packaging plastics: a review, Macromol. Rapid Commun. 42 (2021), https://doi.org/10.1002/marc.202000415.
[9] E. Velásquez, M. Guerrero Correa, L. Garrido, A. Guarda, M.J. Galotto, C. López de Dicastillo, Food packaging plastics: Identification and Recycling (2021) 311–343, https://doi.org/10.1007/978-981-16-3627-1_14.
[10] B. von Vacano, O. Reich, G. Huber, G. Türkoglu, Elucidating pathways of polypropylene chain cleavage and stabilization for multiple loop mechanical recycling, J. Polym. Sci. 61 (2023) 1849–1858, https://doi.org/10.1002/pol.20230121.
[11] V.S. Cecon, P.F. Da Silva, G.W. Curtzwiler, K.L. Vorst, The challenges in recycling post-consumer polyolefins for food contact applications: a review, Resour. Conserv. Recycl. 167 (2021) 105422, https://doi.org/10.1016/j.resconrec.2021.105422.
[12] L. Wu, B. Mu, H. Yang, F. Zhao, Y. Zhu, A. Wang, Fabrication of multifunctional carbon/clay nanocomposites by recycling oil shale semi-coke waste for coloring and enhancing mechanical and aging-resistant properties of

acrylonitrile–butadiene–styrene, Materials Today Sustainability 20 (2022) 100259, https://doi.org/10.1016/j.mtsust.2022.100259.
[13] Y. Xue, Y. Wang, Y. Wang, X. Sui, W. Liang, F. Wang, A superhydrophobic Fe3O4/PEI nanocomposite film with active activation function for anti-icing/deicing applications, Materials Today Sustainability (2023) 100588, https://doi.org/10.1016/j.mtsust.2023.100588.
[14] C. López de Dicastillo, E. Velásquez, A. Rojas, A. Guarda, M.J. Galotto, The use of nanoadditives within recycled polymers for food packaging: properties, recyclability, and safety, Compr. Rev. Food Sci. Food Saf. 19 (2020) 1760–1776, https://doi.org/10.1111/1541-4337.12575.
[15] K. Zdiri, A. Elamri, M. Hamdaoui, O. Harzallah, N. Khenoussi, J. Brendlé, Reinforcement of recycled pp polymers by nanoparticles incorporation, Green Chem. Lett. Rev. 11 (2018) 296–311, https://doi.org/10.1080/17518253.2018.1491645.
[16] FDA Code of Federal Regulations Title 21CFR172.480, Food additives permitted for direct addition to food for human consumption. Title 21, Volume 3. Subpart B Anticaking agents 172.480, (n.d.). https://www.ecfr.gov/current/title-21/chapter-I/subchapter-B/part-172/subpart-E/section-172.480 (accessed November 8, 2023).
[17] U. Okoli, K. Rishi, G. Beaucage, H.K. Kammler, A. McGlasson, M. Chauby, V. Narayanan, J. Grammens, V.K. Kuppa, Dispersion of modified fumed silica in elastomeric nanocomposites, Polymer (Guildf) 264 (2023) 125407, https://doi.org/10.1016/j.polymer.2022.125407.
[18] E. Velásquez, C. López de Dicastillo, C. Patiño Vidal, G. Copello, C. Reyes, A. Guarda, M.J. Galotto, Feasibility of valorization of post-consumer recycled flexible polypropylene by adding fumed nanosilica for its potential use in food packaging toward sustainability, Polymers 15 (2023) 1081, https://doi.org/10.3390/POLYM15051081/S1.
[19] E. Velásquez, S. Espinoza, X. Valenzuela, L. Garrido, M.J. Galotto, A. Guarda, C. López de Dicastillo, Effect of organic modifier types on the Physical–mechanical properties and overall migration of post-consumer polypropylene/clay nanocomposites for food packaging, Polymers 13 (2021), https://doi.org/10.3390/polym13091502.
[20] EC Regulation, Commission Regulation (EU) 2020/1245 of 2 September 2020 amending and correcting Regulation (EU) No 10/2011 on plastic materials and articles intended to come into contact with food (Text with EEA relevance), Off. J. Eur. Union L288 (2020) 1–17.
[21] EFSA Panel on Food Contact Materials. Enzymes, Flavourings and Processing Aids (CEF), Safety assessment of the substance montmorillonite clay modified by dimethyldialkyl (C16-C18) ammonium chloride for use in food contact materials, EFSA J. 13 (2015) 4285, https://doi.org/10.2903/j.efsa.2015.4285.
[22] E. Velásquez, L. Garrido, X. Valenzuela, M.J. Galotto, A. Guarda, C. López de Dicastillo, Valorization of post-consumer recycled polypropylene through their reinforcement with amine and amine/silane organically modified clays for potential use in food packaging, Food Packag. Shelf Life 38 (2023), https://doi.org/10.1016/j.fpsl.2023.101121.
[23] X. Hao, J. Xu, H. Zhou, W. Tang, W. Li, Q. Wang, R. Ou, Interfacial adhesion mechanisms of ultra-highly filled wood fiber/polyethylene composites using maleic anhydride grafted polyethylene as a compatibilizer, Mater. Des. 212 (2021) 110182, https://doi.org/10.1016/j.matdes.2021.110182.
[24] V. Çavuş, Selected properties of mahogany wood flour filled polypropylene composites: the effect of maleic anhydride-grafted polypropylene (MAPP), Bioresources 15 (2020) 2227–2236, https://doi.org/10.15376/biores.15.2.2227-2236.
[25] P. Pathak, S. Sharma, S. Ramakrishna, Circular transformation in plastic management lessens the carbon footprint of the plastic industry, Materials Today Sustainability 22 (2023) 100365, https://doi.org/10.1016/j.mtsust.2023.100365.
[26] V. Titone, M.C. Mistretta, L. Botta, F.P. La Mantia, Investigation on the properties and on the photo-oxidation behaviour of polypropylene/fumed silica nanocomposites, Polymers 13 (2021) 2673, https://doi.org/10.3390/POLYM13162673, 2673 13 (2021.
[27] E. Velásquez, C. Patiño Vidal, G. Copello, C. López de Dicastillo, C.J. Pérez, A. Guarda, M.J. Galotto, Developing post-consumer recycled flexible polypropylene and fumed silica-based nanocomposites with improved processability and thermal stability, Polymers 15 (2023), https://doi.org/10.3390/polym15051142.
[28] D. Li, L. Zhou, X. Wang, L. He, X. Yang, Effect of crystallinity of polyethylene with different densities on breakdown strength and conductance property, Materials 12 (2019) 1746, https://doi.org/10.3390/MA12111746.
[29] G.P.M. de Souza, E.G.R. Dos Anjos, L.S. Montagna, O. Ferro, F.R. Passador, A new strategy for the use of post-processing vacuum bags from aerospace supplies: nucleating agent to LLDPE phase in PA6/LLDPE blends, Recycling 4 (2019) 18, https://doi.org/10.3390/RECYCLING4020018.
[30] H.S. Kim, B.H. Lee, S.W. Choi, S. Kim, H.J. Kim, The effect of types of maleic anhydride-grafted polypropylene (MAPP) on the interfacial adhesion properties of bio-flour-filled polypropylene composites, Compos Part A Appl Sci Manuf 38 (2007) 1473–1482, https://doi.org/10.1016/J.COMPOSITESA.2007.01.004.
[31] G. Dikobe, A.S. Luyt, Comparative study of the morphology and properties of PP/LLDPE/wood powder and MAPP/LLDPE/wood powder polymer blend composites, Express Polym. Lett. 4 (2010) 729–741, https://doi.org/10.3144/expresspolymlett.2010.88.
[32] G.S. Ezat, A.L. Kelly, S.C. Mitchell, M. Youseffi, P.D. Coates, Effect of maleic anhydride grafted polypropylene compatibilizer on the morphology and properties of polypropylene/multiwalled carbon nanotube composite, Polym. Compos. 33 (2012) 1376–1386, https://doi.org/10.1002/pc.22264.
[33] H. Nasution, S. Pandia, Maulida, M.S. Sinaga, Impact strength and thermal degradation of waste polypropylene (wPP)/Oil palm empty fruit bunch (OPEFB) composites: effect of maleic anhydride -g-polypropylene (MAPP) addition, Procedia Chem. 16 (2015) 432–437, https://doi.org/10.1016/j.proche.2015.12.075.
[34] D. Jubinville, C. Tzoganakis, T.H. Mekonnen, Simulated recycling of polypropylene and maleated polypropylene for the fabrication of highly-filled wood plastic composites, ACS Appl. Polym. Mater. 4 (2022) 2373–2383, https://doi.org/10.1021/acsapm.1c01671.
[35] E. Velásquez, L. Garrido, X. Valenzuela, M.J. Galotto, A. Guarda, C. López de Dicastillo, Physical properties and safety of 100% post-consumer PET bottle -organoclay nanocomposites towards a circular economy, Sustain Chem Pharm 17 (2020) 100285, https://doi.org/10.1016/J.SCP.2020.100285.
[36] M. Gómez, D. Bracho, H. Palza, R. Quijada, Effect of morphology on the permeability, mechanical and thermal properties of polypropylene/SiO_2 nanocomposites, Polym. Int. 64 (2015) 1245–1251, https://doi.org/10.1002/pi.4909.